Lecture 10: Linear Inverse Heat Conduction Problems-Two basic examples

Y. Jarny[2], D. Maillet[1]

[1] LEMTA, Nancy-University & CNRS, Vandoeuvre-lès-Nancy, France
E-mail: denis.maillet@ensem.inpl-nancy.fr
[2] LTN, Nantes-University & CNRS , Nantes, France
E-mail: yvon.jarny@polytech.univ-nantes.fr

Abstract. Two basic examples of Linear Inverse Heat Conduction Problems (LIHCP) are presented. They aims both to determine the time varying heat flux density entering a solid wall, from noisy data given by some measurements of the temperature rise inside the wall. In the first case, the wall is assumed to be a semi-infinite body, the second case is the standard plane wall. The instabilities of the numerical solutions are analyzed. The influences of the level noise, the sensor locations, the time step are investigated. The use of the spectral value decomposition (SVD) of the linear operator to build regularized solutions is also illustrated.

1. Introduction

How to determine the time varying heat flux density entering a solid wall, from noisy data given by some temperature measurements inside the wall, is a very standard Inverse Heat Conduction Problems (IHCP), and the choice in practice of a numerical method for solving such problems is not obvious, it will depend on the complexity of the model equations: are they linear or not? What is the dimension? What is the shape of the spatial domain? In any case, some specific difficulties are "expected", because IHCP are known to be ill-conditioned and regularized processes have to be developed for avoiding instable solutions due to noisy data.
In this lecture we considered two basic examples of linear IHCP: in the first case, the wall is assumed to be a semi-infinite body, and the second case is the standard plane wall. By investigating the model equations, it is possible to exhibit the matrix form of the linear operator to be inversed. We are more interested in the analysis of the instabilities than in the development of the regularization methods. For such linear problems, it will be shown how the spectral value decomposition (SVD) of the linear operator is a powerful approach.

2. Semi-infinite heat conduction body

2.1- The model equations

The semi-infinite solid is a simple geometry for which analytical solutions of the heat conduction equation may be obtained. Since such a solid extends to infinity in all but one direction, it is characterized by a single identifiable surface. If a sudden change of condition is imposed at this surface, transient, one-dimensional conduction occur within the solid. This configuration provides a useful idealization for many practical problems [1].

Let us consider a semi-infinite body in the axis direction x, which receives the heat flux density u(t) (W.m-2), on the boundary x = 0, at the initial time t = 0. The spatial distribution of the initial temperature field T_0 (x) can be non uniform. A temperature sensor is located at x_c

The temperature field *T(x,t)*, solution of the heat conduction equation, depends on the physical parameters: thermal conductivity λ ($W.m^{-1}.K^{-1}$), heat diffusivity $a = \lambda / \rho c$ ($m^2.s^{-1}$) and thermal effusivity $b = (\lambda \rho c)^{1/2}$

The output signal of the modeling equations is:

$$y_{mo}(t) = T(x_c, t) \tag{1a}$$

By introducing:

- the Green function

$$G(x_c, x, t) = \frac{1}{2\sqrt{\pi a t}}\left[\exp\left(-\frac{(x_c - x)^2}{4 a t}\right) + \exp\left(-\frac{(x_c + x)^2}{4 a t}\right)\right] \tag{1b}$$

- and the impulse response $Z(t) = \frac{1}{b\sqrt{\pi t}} \exp\left(-x_c^2 / 4at\right)$ (1c)

the output can be written as the sum of two terms

$$y_{mo}(t) = \int_0^{\infty} G(x_c, x, t)\, T_0(x)\, dx + \int_0^t Z(t-\tau)\, u(\tau)\, d\tau = y_{mo\ relax}(t) + y_{mo\ forced}(t) \tag{2}$$

The first term $y_{mo\ relax}(t)$ corresponds to the relaxation of the initial field, it vanishes for long time, the second term $y_{mo\ forced}(t)$ is the thermal response expressed as the result of the convolution of the input signal heat flux *u(t)*, with the impulse response *Z(t)*

When the initial field is assumed to be uniform, equal to T_0, then the first term remains equal to T_0, and the output signal becomes

$$y_{mo}(t) = T(x_c, t) - T_0 = \int_0^t Z(t-t')\, u(t')\, dt' \tag{3}$$

Rewriting the impulse response as:

$$Z(t) = K\sqrt{\frac{\tau}{t}} \exp\left(-\frac{\tau}{t}\right) \quad \text{with} \quad \tau = \frac{x_c^2}{4a} \quad \text{and} \quad K = \frac{2}{\rho c\, x_c \sqrt{\pi}}$$

and considering the input as a (unitary) impulse,

$$u_\delta(t) = Q\,\delta(t) \quad \text{with} \quad Q = 1\ \mathrm{Jm^{-2}} \quad \text{and} \quad \int_0^{\infty} \delta(t)\, dt = 1$$

the plot of the impulse output $Z^*(t) = Z(t)/K$ (with $T_0 = 0$) versus the reduced time $t^* = \frac{t}{\tau}$ is shown on figure 1. It must be noted that the characteristic time to reach the maximum value is given by

$$t_m = 2\tau = \frac{x_c^2}{2a},$$

During experiments which lead to temperature measurements, this typical value has to be reminded to choose correctly the data acquisition time step Δt, in practice it must be chosen in order to satisfy $\Delta t << \tau$.

The discrete output response $y_{mo}(\mathrm{t}_i), \mathrm{i} = 1,2,...$ to any arbitrary input $u_i = u(\mathrm{t}_i), \mathrm{i} = 1,2,...$ can be then approximated from a numerical solution of equation (3):

$$y_{mo}(\mathrm{t}_i) = \Delta t \sum_{j=1}^{i} Z\,(t_i - t_{j-1})\,u_j = \sum_{j=1}^{i} \mathrm{S}_{\mathrm{i}\,\mathrm{j}}\,u_j \qquad (4a)$$

$$\mathrm{S}_{\mathrm{i}\,\mathrm{j}} = \begin{cases} \Delta t\; Z\left((\mathrm{i} - j + 1)\,\Delta t\right) = z_{i-j+1} & \text{for} \quad j = 1\ à\ i \quad \text{and} \quad i = 1\ à\ m \\ 0 \quad \text{else} \end{cases} \qquad (4b)$$

which can be written in the linear matrix form : $\mathbf{y}_{mo} = \mathbf{S}\,\mathbf{u}$ (4c)

S is a Toeplitz matrix, and takes the specific triangular form

$$\boldsymbol{S} = \begin{bmatrix} z_1 & 0 & & & \\ z_2 & z_1 & 0 & & 0 \\ z_3 & z_2 & z_1 & & \\ z_4 & z_3 & z_2 & \ddots & 0 \\ & & & \ddots & z_1 \quad 0 \\ z_m & z_{m-1} & z_{m-2} & & z_2 \quad z_1 \end{bmatrix} \qquad (4d)$$

Note that the sensitivity coefficients z_i depends on the time step Δt, and goes to zero when $\Delta t \to 0$

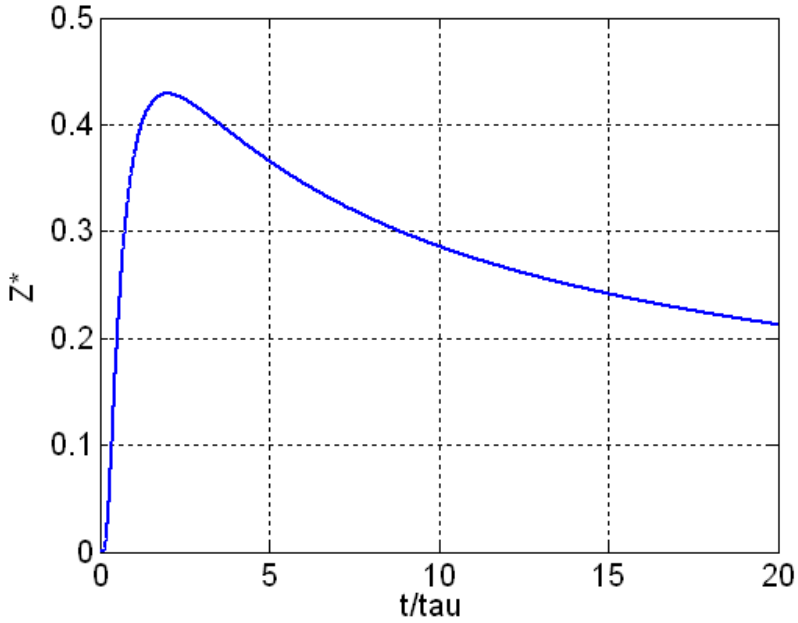

Figure 1 – The impulse output signal - Heat conduction in a semi-infinite body

2.2- The IHCP in a semi-infinite body – a non regularized solution

The inverse heat conduction problem which aims to reconstruct the heat flux signal *u(t)* from the noisy output signal *y*(t) is obviously a time deconvolution problem and the solution is well known to be very sensitive to the noise measurement. Regularized solutions have to be developed.
To illustrate how the inverse problem is ill-conditioned, let us examine first the influence of the level noise on a non regularized solution given by:

$$\hat{\mathbf{u}} = \mathbf{S}^{-1}\mathbf{y} \tag{5}$$

Without loss of generality, we consider the following numerical case:

- the heat flux density *u(t)* is given by the triangular signal, plotted on figure 2, over the time interval $\left[0,\ t_f = 20\ \text{s}\right]$

- the thermal properties and the sensor location are $x_c = 2\ \text{mm}$; $a = 10^{-6}\,\text{m}^2\text{s}^{-1}$; $\tau = 1\ \text{s}$ $\lambda = 1\ \text{W m}^{-1}\,\text{K}^{-1}$ $\rho c = 10^6\ \text{J kg}^{-1}\,\text{K}^{-1}$, $K = 0.564\ 10^{-3}\ \text{K m}^2\,\text{J}^{-1}$.

- The output signal y(t) is plotted on the same figure 2a, it is computed with a time step $\Delta t = 0.5\ \text{s}$, and an additive (zero mean) gaussian noise with $\sigma = 0.005K$

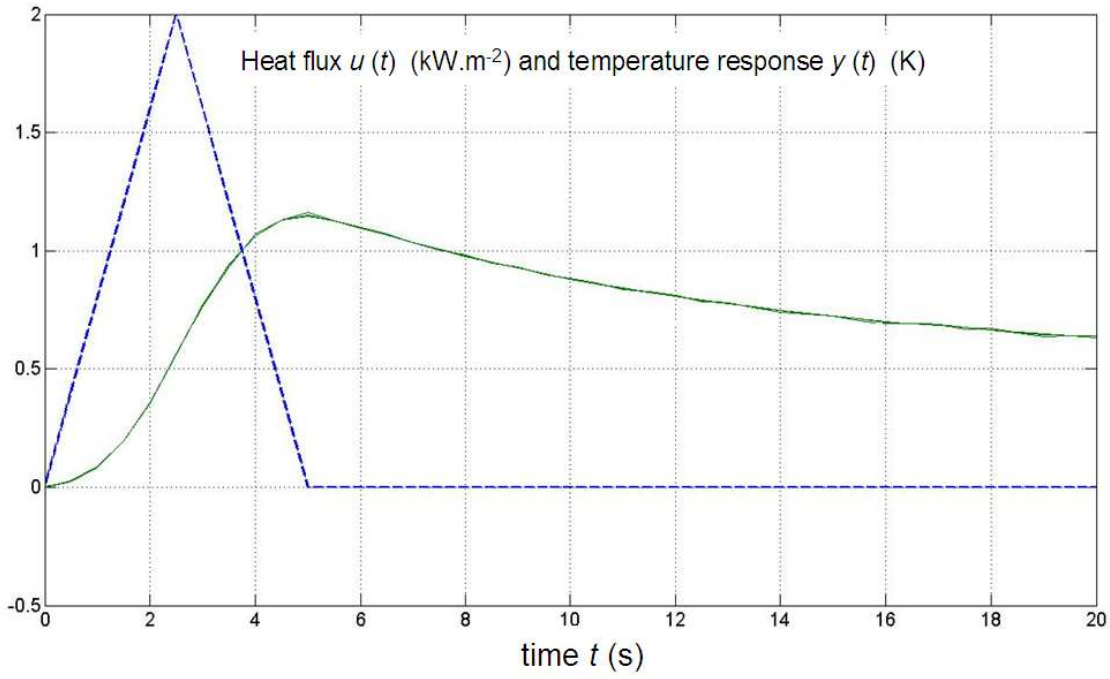

Figure 2a – Input signal *u* (*t*) and output response *y(t)* computed with $\sigma = 0.005K$ and $\Delta t = 0.5$ s

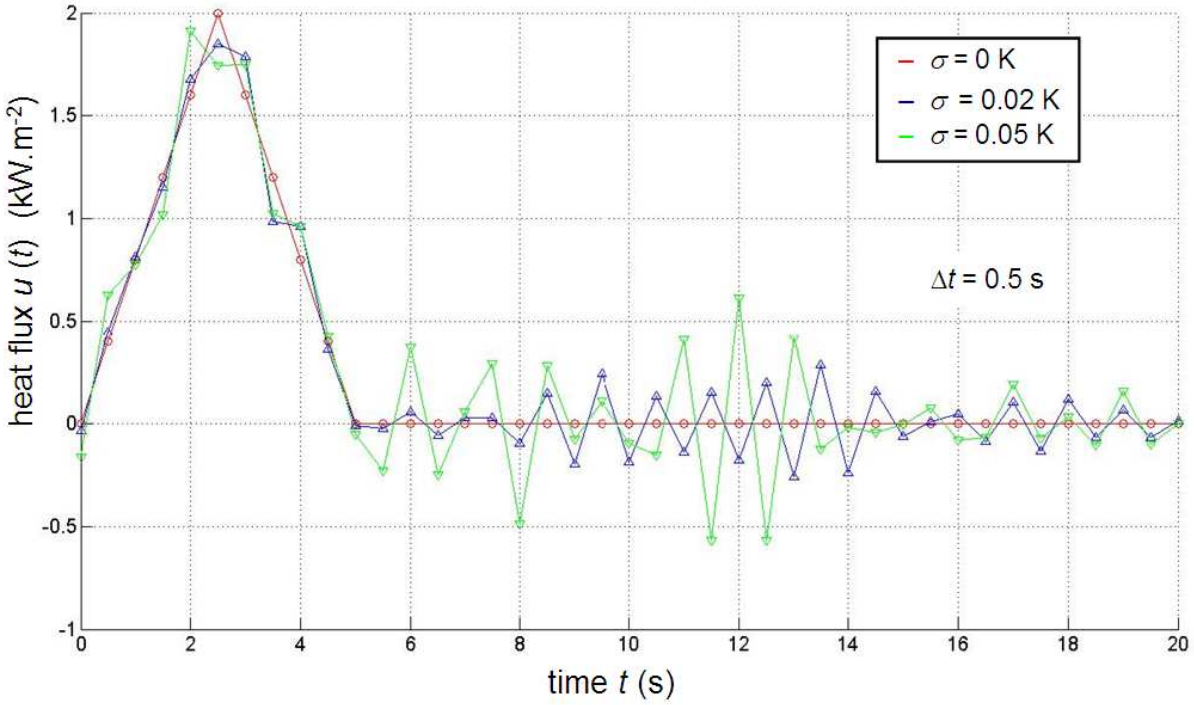

Figure 2b – Estimated heat flux – cases a, b and c - Influence of the noise level on the computed heat flux - time step $\Delta t = 0{,}5\ \mathrm{s}$

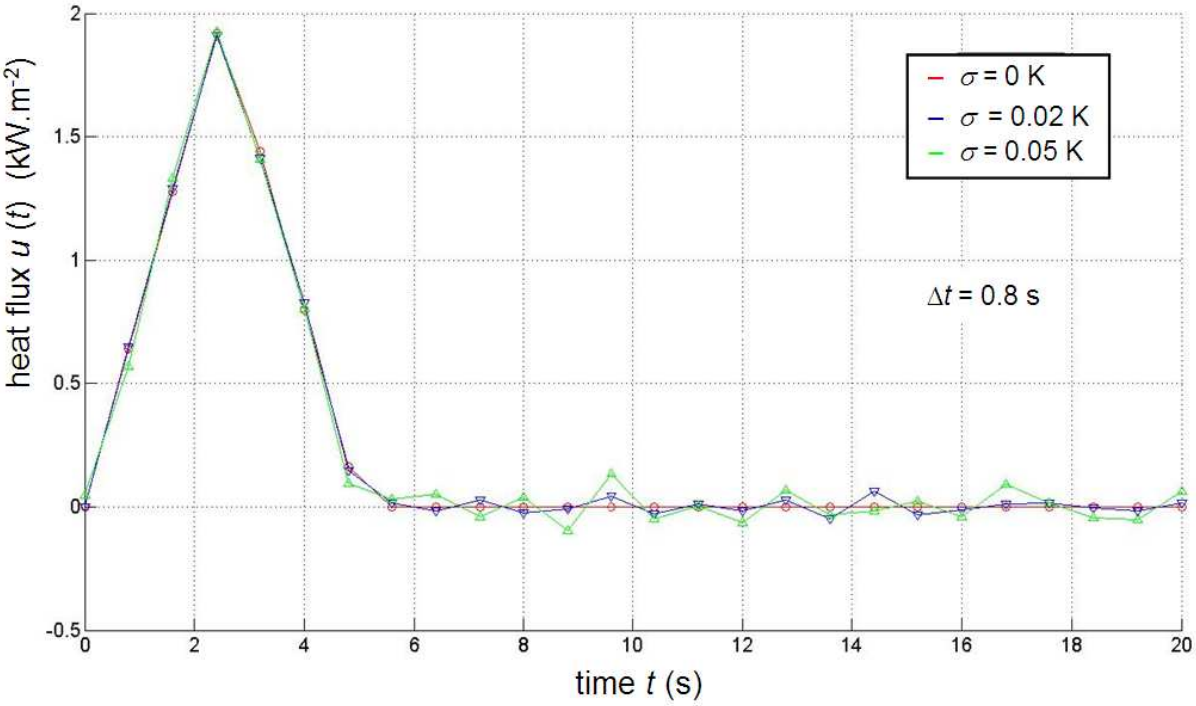

Figure 2c – Estimated heat flux – cases a, b and c - Influence of the noise level on the computed heat flux - time step $\Delta t = 0.8\mathrm{s}$

The computed heat flux, according to equation (5), cases a, b and c, are plotted on figure 2b, for three noise levels ($\sigma = 0{,}0\,;\, 0{,}002$ et $0{,}005$ K), with a time step $\Delta t = 0{,}5$ s

By computing the heat flux, according to equation (5), but with a greater time step $\Delta t = 0{,}8$ s , (now $m = 20$), and for the same noise levels σ , the numerical solutions are plotted on figure 2c.

The comparison of the inversion results, case b and case c, show that by increasing the time step, the solution becomes less sensitive to the noise measurement. This numerical phenomena is not specific to that example, it is "generic" for this kind of inverse problem.

To increase the accuracy of the numerical approximation of the solution of the forward problem, the time step is usually decreased. It must be observed here that decreasing the time step leads to make the solution of the inverse problem less stable.

In fact by decreasing the time step, the sensitivity coefficients of the Toeplitz matrix S , equation (4c), goes to zero, and the condition number grows exponentially:

Table 1 – Condition number of the matrix ***S*** – IHCP in a semi-infinite body

Δt	$\Delta t = 0{,}8$ s	$\Delta t = 0{,}5$ s	$\Delta t = 0{,}4$ s	
Cond(S)	46,5	292	28420	

Then by decreasing the time step, the inversion process of the noised data leads to more and more unstable solutions. On the contrary, by increasing the time step, some "regularization" process occurs, the computed solution becomes more stable, but of course this is done by decreasing the accuracy of the solution. Some compromises have to be searched for.

2.3- The IHCP in a semi-infinite body- Influence of the time step

In this example, another simple analysis of the influence of the time step Δt on the stability of the inversion process of noisy data can be derived directly from the model equations and the output noise level.

As shown on figure 2.a, for $t < 5$ the heat flux density signal is triangular, the slope (800 $Wm^{-2}s^{-1)}$ is known, so the mean value of the increment $|\Delta u(t)|$ on each time step $[\, t_k \; t_k + \Delta t \,]$ satisfies

$$\Delta u = \frac{1}{\Delta t} \int_{t_k}^{t_k + \Delta t} 800\; t \; \mathrm{d}t = 400\, \Delta t \tag{6a}$$

The resulting increment on the output signal can be approximated by

$$\Delta y \approx \; K \Delta \mathrm{t} \sqrt{\frac{\tau}{\Delta \mathrm{t}}} \; \exp(-\tau / \Delta t) \Delta \mathrm{u} \tag{6b}$$

This increment of the output signal will be "significant" only if this value is greater than the level noise : $\Delta y > \sigma$. In this example, we have: $K = 0.564\, 10^{-3}$ K m^2 J^{-1}, $\tau = 1$ s , $\sigma = 0.005 K$, then we get :

$$\Delta y = \; 0.564 * 400 * (\Delta t)^2 \sqrt{\frac{1}{\Delta t}} \; \exp(-1/\Delta t) \geq \sigma$$
$$\Rightarrow 0.225(\Delta t)^{3/2} \exp(-1/\Delta t) \geq \sigma \qquad (6c)$$

By plotting the variation of the increment Δy versus the time step Δt, figure 3, it is observed that

- for Δt = 0.8s, the output increment Δy =46,3mK is much larger than the level noise,
- for Δt = 0.5s, Δy > 0.01mK is only twice more than the level noise
- for Δt = 0.4 s. Δy =4,7mK becomes less than the level noise $\sigma = 5mK$.

Of course, these values are specific to this numerical example, but they could be computed for other examples of semi-infinite heat conduction problem with different values of thermal parameters, and/or sensor location. They well explain how increasing the time step Δt contributes to the stability of the numerical solutions of the inverse problem.

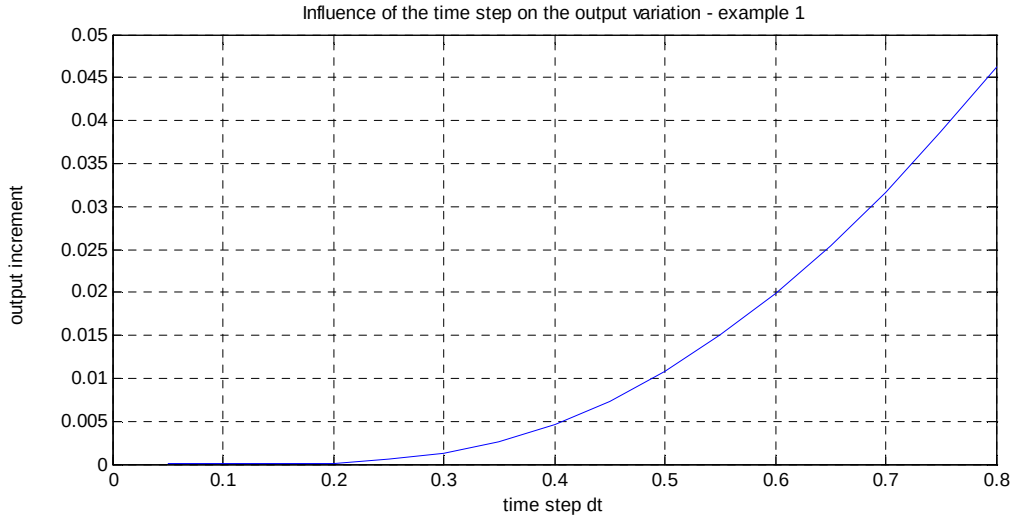

Figure 3: Output increment Δy versus time step Δt – semi-infinite conduction model

2.4- The IHCP in a semi-infinite body – a regularized solution

The inverse heat conduction problem being linear, the spectral value decomposition (SVD) analysis of the sensitivity matrix is a powerful method to determine a regularized solution.

For example, the solution $\hat{u} = \mathbf{S}^{-1} y$, computed without regularization, with a time step $\Delta t = 0{,}4\,\mathrm{s}$ and plotted figure (3), illustrates how the noise of the output data is amplified, and the need of some regularization.

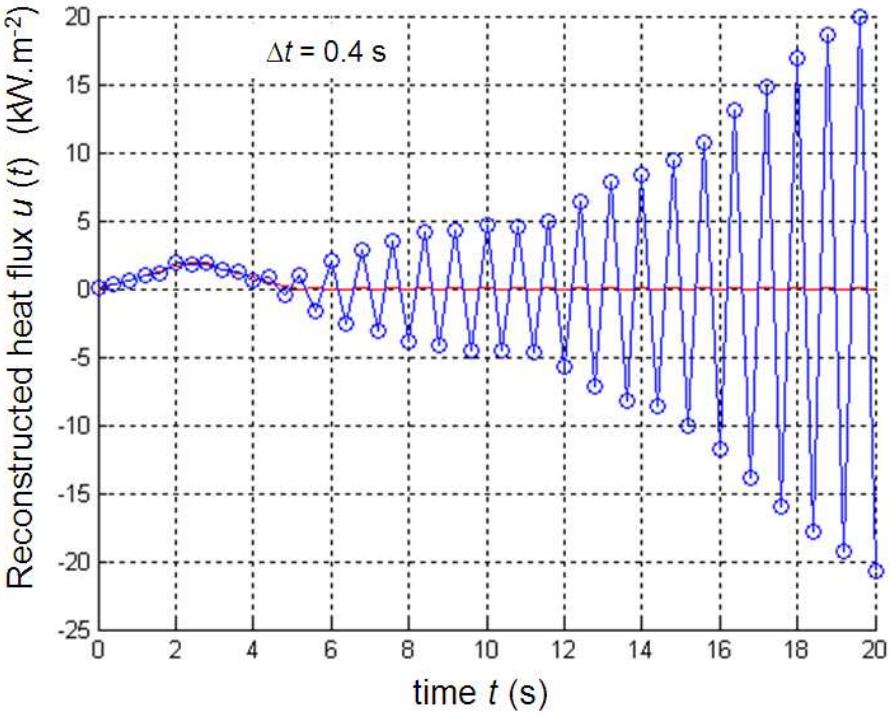

Figure 4
Heat flux $u(t)$ computed without regularization ($\hat{u} = S^{-1} y$), from noised data $\sigma = 0{,}005$ K, for a time step $\Delta t = 0{,}4$ s

The use of the SVD method is straightforward:

- the sensitivity matrix is first decomposed in the form

$$\boldsymbol{S} = \boldsymbol{U}\,\boldsymbol{W}\,\boldsymbol{V}^{T} \tag{7}$$

where $\boldsymbol{U}$, $\boldsymbol{V}$ are orthogonal matrices
and $\boldsymbol{W}$ is the matrix of the singular values $\{w_k, k = 1,..m\}$
In this example, the matrices are squared and their size is $m = n = 51$

- The SVD regularized solution is then

$$\hat{\mathbf{u}}_r = \sum_{k=1}^{r<n} \frac{a_k}{w_k}\,\mathbf{V}_k \quad with \quad a_k = \mathbf{U}_k^T\,\mathbf{y} \tag{8}$$

The « hyper-parameter » r is used to decide of the "good regularization level". The expected compromise between accuracy and stability is fixed by some optimal value of r. We have to avoid:

- a too big error amplification when $k \to m$, because $w_k \to 0$, hence $\frac{a_k}{w_k} \to \infty$
- A too large bias when $k \to 0$, because all the components $\{a_k = \mathbf{U}_k^T y, k = r+1,.., m\}$ of the output noisy data are ignored, only the components $\{a_k = \mathbf{U}_k^T y, k = 1,.., r\}$ are taken into account.

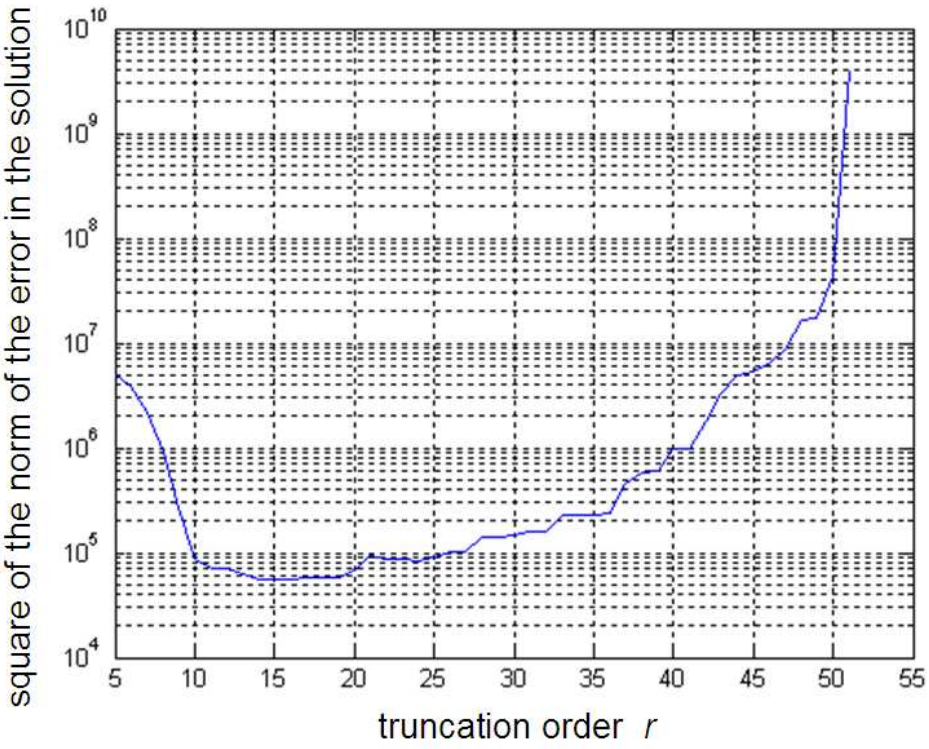

Figure 5 - Quadratic error $f(r) = \left\| \hat{\boldsymbol{u}}_r - \boldsymbol{u} \right\|^2$ versus r ($\Delta t = 0{,}4$ s, $\sigma = 0{,}005$ K), $m = 51$

It is possible (in this example) to compute the exact solution $\boldsymbol{u}^*$, and for each value of r, the regularized one $\hat{\boldsymbol{u}}_r$. Then the quadratic error $f(r) = \left\| \hat{\mathbf{u}}_r - \mathbf{u}^* \right\|^2$ can be plotted versus r, figure 4. It is observed that a minimum is reached in the neighborhood of $r = 15$.

The heat flux computed with $r = 12, 15$ et 18 are plotted on the figure 6. Compared to the non regularized solution (figure 4), we conclude on the efficiency of this method: the solutions are stable, even for $\Delta t = 0{,}4$ s and $\sigma = 0{,}005$ K. However a slight bias is observed, (see the figure 2a), the peak value is less than the exact value (= 2 Wm^{-2}).

Other standard methods are well adapted and can be used for solving such linear inverse heat conduction problems, the well known Beck's method (sequential algorithms), or the conjugate gradient algorithm [3] are recommended and give good results.

In practice, the exact solution is unknown, then the determination of the optimal SVD truncation cannot be done by searching for the minimum of $f(r) = \left\| \hat{\mathbf{u}}_r - \mathbf{u}^* \right\|^2$.

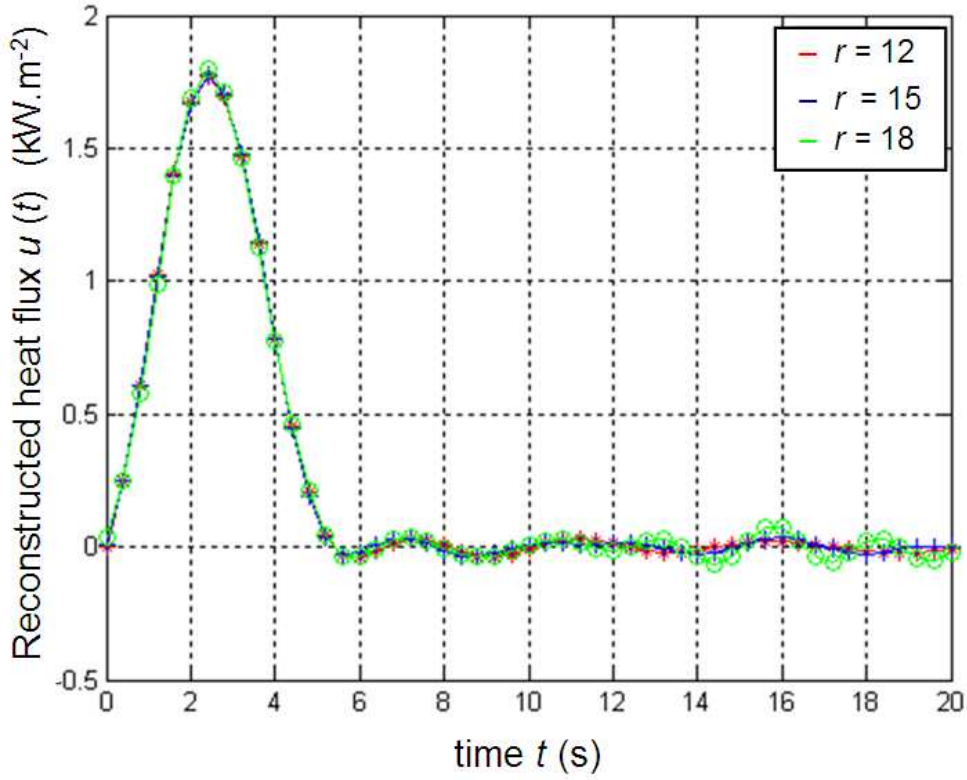

Figure 6 - SVD Regularized Heat flux $\hat{\boldsymbol{u}}_r$ computed for $r = 12, 15$ et 18
$(\Delta t = 0{,}4\ \text{s}, \sigma = 0{,}005\ \text{K})$

Some bound of the error estimate $\mathbf{e}_u = \hat{\mathbf{u}}_r - \mathbf{u}^*$, has to be *a priori* given to select the best truncation order *r*. A "L-curve" approach (see lecture L9) can also be developed.

However, a more detailed analysis can be done. Let us denote $c = m - r$, $\boldsymbol{\varepsilon}$ the additive noise and

$$\mathbf{U} = \left[\mathbf{U}^r \ \ \mathbf{U}^c\right] ; V = \left[V^r \ \ V^c\right]; \ \mathbf{W} = \begin{bmatrix} \mathbf{W}^r & \mathbf{0} \\ \mathbf{0} & \mathbf{W}^c \end{bmatrix} \quad \text{and} \quad \mathbf{u} = \begin{bmatrix} \mathbf{u}^r \\ \mathbf{u}^c \end{bmatrix} \tag{9}$$

Then, the error estimate can be put in the form

$$\boldsymbol{e}_u = \boldsymbol{V}^r \left(\boldsymbol{W}^r\right)^{-1} \left(\boldsymbol{U}^r\right)^T \boldsymbol{\varepsilon} - \boldsymbol{V}^c \ \hat{\boldsymbol{u}}_c^* \tag{10}$$

which leads to

$$\mathrm{E}\left(\boldsymbol{e}_u{}^T \boldsymbol{e}_u\right) = \sigma^2 \sum_{i=1}^{r} \frac{1}{w_k^2} + \sum_{k=r+1}^{m} \hat{u}_k^{*\,2} \tag{11}$$

- The first term is directly linked to the variance of the measurement noise, it increases by increasing the truncation parameter *r*,
- and the second term depends only on the $c = m - r$ spectral components of the exact heat flux signal, which have been "lost" by truncation.

It means that the ill-conditioning of the inverse heat conduction problem depends both on the mathematical model equations (singular values w_j of matrix $\boldsymbol{S}$), and on the spectral values of the input signal to be determined. The compromise in choosing the parameter r takes into account these both contributions.

3. Heat conduction in a Plane wall

3.1- The model equations

One dimensional transient heat conduction is now considered in a plane wall of thickness e, subjected to a convection condition at the boundary $x = e$. Like in the previous example, the wall receives a heat flux density $u(t)$ (W.m-2), on the boundary $x = 0$, at the initial time $t = 0$. For convenience, the initial and ambient temperature field are taken equal to zero $T_0 = T_\infty = 0$

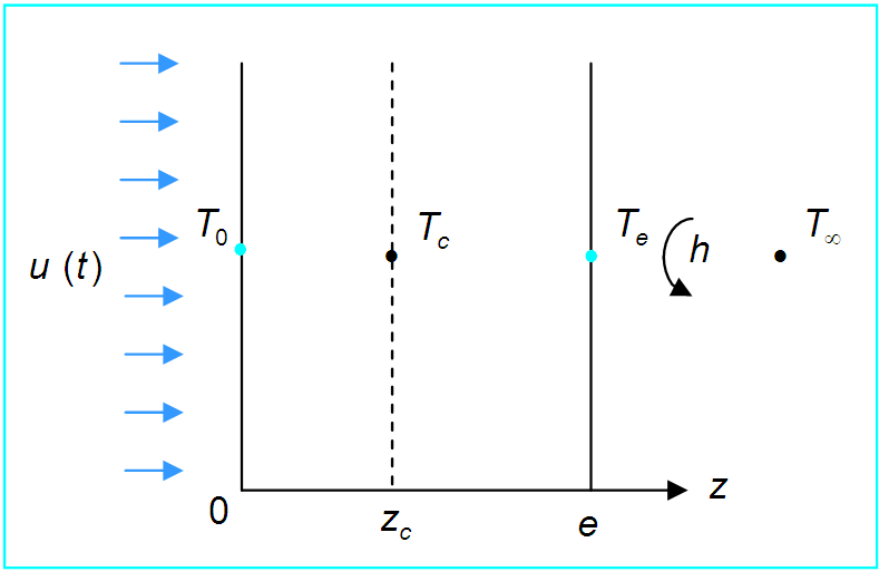

Figure 7 – Transient heat conduction in a plane wall

A standard approximation of the spatial derivatives in the one-dimensional heat conduction equation, with a regular spatial mesh including N nodes, leads to a "state-space" model equations

$$\frac{d\boldsymbol{T}}{dt} = \boldsymbol{A}\,\boldsymbol{T} + \boldsymbol{b}\,u(t) \quad \text{avec} \quad \boldsymbol{T}\,(t=0) = \boldsymbol{0} \tag{12a}$$

where :

$$\mathbf{T}\,(t) = \left[T_1(t) \quad T_2(t) \quad \cdots \quad T_N\,(t)\right]^T \quad \text{avec} \quad T_i\,(t) = T\,(z_i, t)$$
$$\textit{and} \quad z_i = (i-1)\,\Delta z \quad ; \quad \Delta z = \frac{e}{N-1} \tag{12b}$$

$$\boldsymbol{A} = \frac{a}{(\Delta z)^2}\begin{bmatrix} -2 & 2 & 0 & \cdots & 0 \\ 1 & -2 & 1 & & 0 \\ \vdots & & \ddots & & \vdots \\ & & & -2 & 1 \\ 0 & 0 & \cdots & 2 & -2(1+Bi) \end{bmatrix} \quad \text{et} \quad \boldsymbol{b} = \frac{2}{\rho c\ \Delta z}\begin{bmatrix} 1 \\ 0 \\ \vdots \\ 0 \\ 0 \end{bmatrix} \tag{12c}$$

$$Bi = h\ \Delta z / \lambda \quad \text{(Mesh Biot number)} \tag{12d}$$

A temperature sensor is assumed to be located at $z_c = (i_c - 1)\ \Delta z$. The output equation of the model takes the matrix form

$$\mathbf{y}_{mo}(t) = \mathbf{C}\ \mathbf{T}(t) \qquad \text{with} \quad \mathbf{C} = [0 \quad 0 \quad \cdots \quad 1 \quad \cdots \quad 0] \ \text{ where } \ C_i = 0 \ \text{ si } \ i \neq i_c \tag{13}$$

and the output signal $\mathrm{y}_{mo}(t)$ is given by

$$\mathrm{y}_{mo}(t) = \mathbf{C} \int_0^t \mathbf{exp}\,(\mathbf{A}\,(t-\tau))\ \mathbf{b}\ u(\tau)\ \mathrm{d}\tau \tag{14a}$$

At $t_k = k\ \Delta t\ , k = 1,..,n_t$ the discretized output is given by:

$$\mathrm{y}_{mo}(t_k) = \mathbf{C} \int_0^{t_k} \mathbf{exp}\,(\mathbf{A}\,(t_k-\tau))\ \mathbf{b}\ u(\tau)\ \mathrm{d}\tau \qquad \text{for} \qquad k = 1, 2, \cdots, n \tag{14b}$$

Let us introduce the parameterized form of the input signal

$$u(t) \approx u_{\text{param}}(t) = \sum_{j=1}^{n} u_j\ f_j(t) \tag{15}$$

Then, the input-output model equation takes the same linear matrix equation than in the previous example

$$\mathbf{y}_{mo} = \mathbf{S}\ \mathbf{u} \qquad \text{with} \quad y_{mo,k} = \mathrm{y}_{mo}(t_k)$$

$$\mathrm{y}_{mo}(t_k) = \sum_{j=1}^{n} S_{kj}\ u_j; \qquad S_{kj} = \mathbf{C} \int_0^{t_k} \mathbf{exp}\,(\mathbf{A}\,(t_k-\tau))\ \mathbf{b}\ f_j(\tau)\ \mathrm{d}\tau \tag{16}$$

3.2- Numerical example - Influence of the sensor locations

Numerical results are obtained with the following data:
$e = 0{,}05$ m; $\lambda = 0{,}3$ $\mathrm{Wm^{-1}K^{-1}}$; $\rho c = 1.2\ 10^6$ $\mathrm{Jm^{-3}K^{-1}}$, and $h = 0$ $\mathrm{Wm^{-2}K^{-1}}$.
The chosen input heat flux is plotted on the figure xx
The output signal $y_{mo}(t)$ is computed at three different locations $z_c = e/4;\ e/2;\ 3e/4$, over the time interval $[0,\ t_f = 8000\ \mathrm{s}]$, with $N = 21$ nodes et $n_t = 40$ time steps ($\Delta t = 200s$), the output

are plotted on the same figure xx. The node numbers which corresponds to the sensor locations are then $i_c \in \{6, 11, 16\}$. An additive (zero mean) Gaussian noise ε, with $\sigma = 0{,}02\ K$ is considered:

$$\boldsymbol{y} = \boldsymbol{y}_{mo} + \boldsymbol{\varepsilon} \tag{17}$$

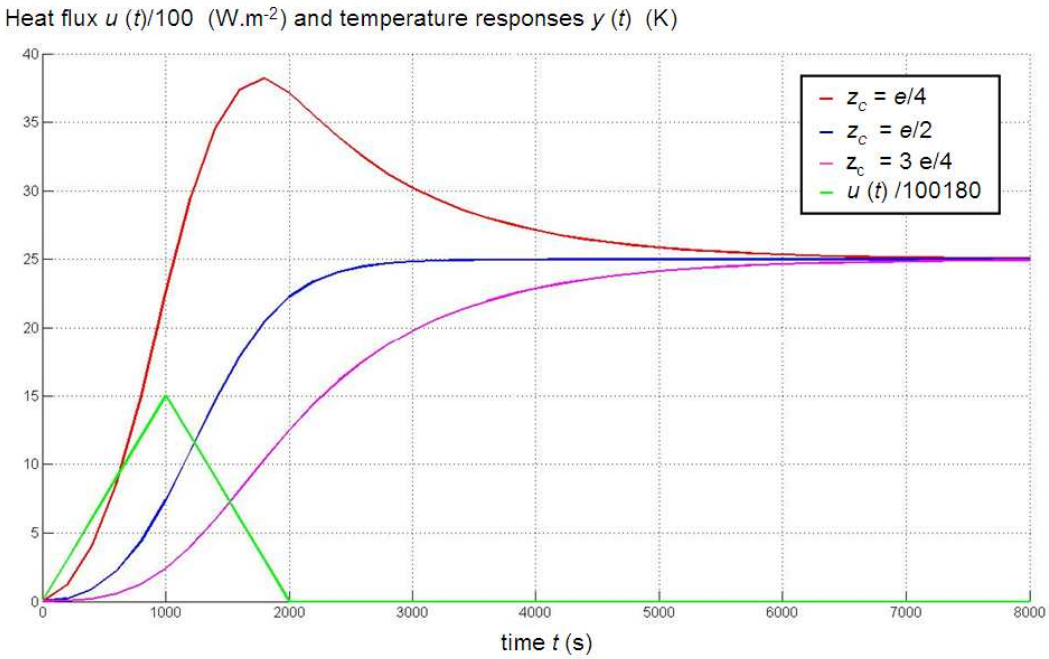

Figure 8 –Input heat flux and output thermal measurements – Plane wall

3.2- The IHCP in a plane wall – non regularized solution

These noised output data are now used to solve the inverse heat conduction problem, which aims to reconstruct the input signal.
A non regularized solution is first computed to illustrate the ill-posedness of the problem

$$\mathbf{S}\,\mathbf{u} = \mathbf{y} \qquad \Rightarrow \qquad \hat{\mathbf{u}} = \mathbf{S}^{-1}\,\mathbf{y} \tag{18}$$

As in the previous example, the influence of the time step on the computed heat flux $\hat{\boldsymbol{u}}$ is shown on the plot, figure 9. Two values are compared : $\Delta t = 200$ s and $\Delta t = 320$ s. Moreover the influence of the sensor locations is also clearly illustrated.

Obviously, as far as the sensor location moves away from the boundary $x = 0$, where the heat flux has to be estimated, the computed solution becomes more and more unstable. Like in the previous example, increasing the time step has a beneficial effect to make the solution less sensitive to noisy data. The ill-posedness of the inverse problem is quantified by the condition number cond ($\boldsymbol{S}$) which grows exponentially with the sensor location, as shown in the following table.

As in the previous example, regularized solutions could be easily computed by using the SVD approach.

Table 2 – Condition number of the matrix ***S*** - IHCP in a plane wall

z_c	e / 4	e / 2	3 e / 4
Δt = 200 s	730	8700	$1{,}0244\ 10^5$
Δt = 320 s	343*	2349	$1{,}7\ 10^4$

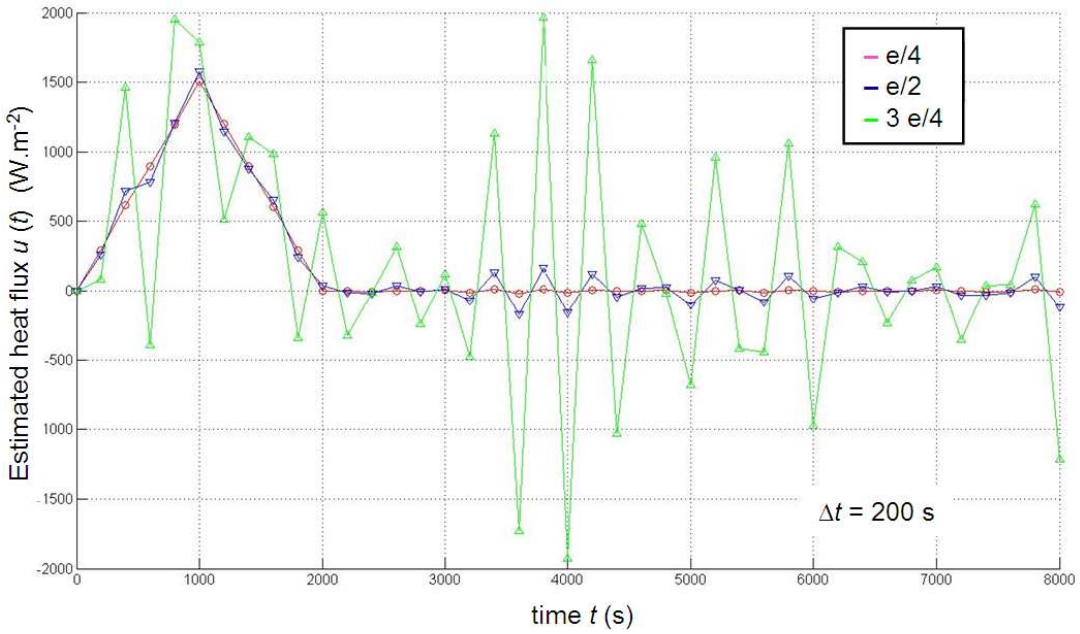

Figure 9b – Estimated heat flux $\hat{\boldsymbol{u}}$ - Influence of the sensor locations **(** Δt = 200 s ; $\sigma = 0{,}02\ K$ **)**

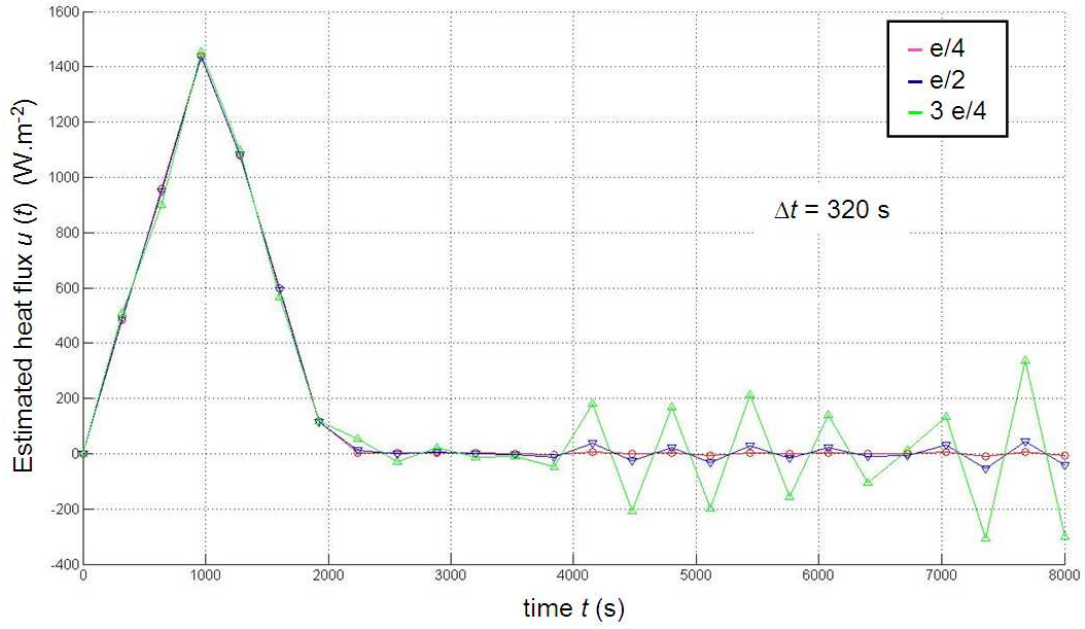

Figure 9c – Estimated heat flux $\hat{\boldsymbol{u}}$ - Influence of the sensor locations **(** Δt = 320 s ; $\sigma = 0{,}02\ K$ **)**

3.3- The IHCP in a plane wall – Effect of a biased model

Up to now, the model equations used to develop the data inversion process, have been assumed to be exact! In practice even for this simple heat conduction model, some model errors may occur.

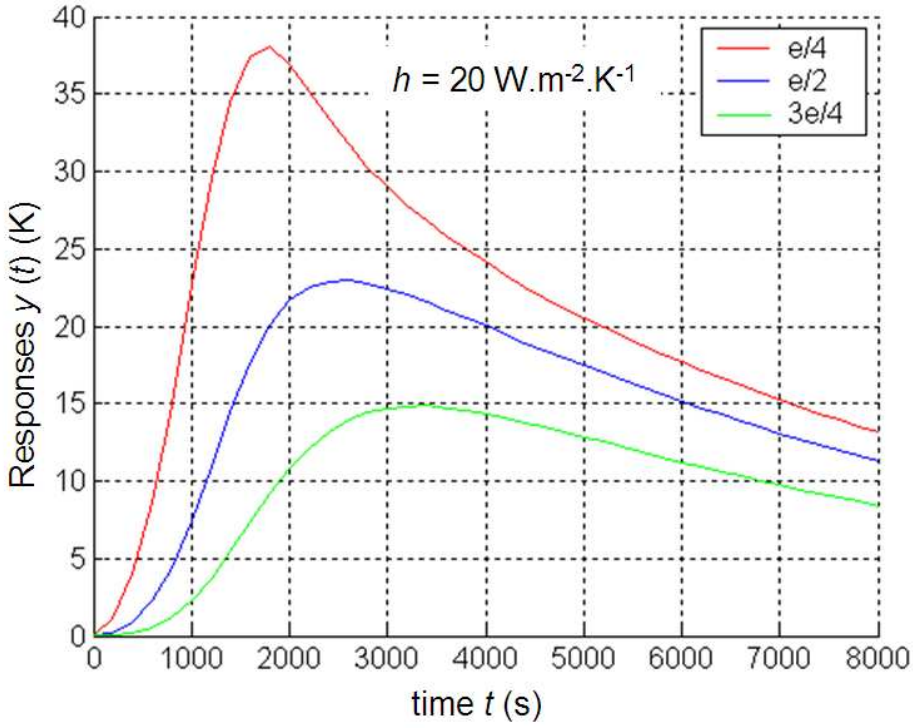

Figure 9d – Heat conduction in a plane wall- Output signal computed with h = 20 W m^{-2} K^{-1}

Suppose, for example, that the heat transfer coefficient of the model equations is h = 20 W m^{-2}K^{-1}, instead of the insulated boundary hypothesis (h = *0).* The value of the Biot number which characterizes the heat losses at the boundary $x = e$, is then Bi = 3,3. The output signals in that case, should be as in the above plot, figure 9d. The Influence of this parameter on the output signal becomes more and more significant (compare with the figure 8), when the sensor is located closer to the boundary $x = e$, where the "wrong" condition occurs.

The numerical inversion process $\hat{\mathbf{u}} = \mathbf{S}^{-1}\mathbf{y}$, is now applied to the same original noisy output data, figure 8, but a model error (h = 20 W m^{-2}K^{-1}), is included in the matrix S.

Numerical results are plotted on figure 9e. The influence of the sensor location is clearly illustrated. There is a systematic error $b_u(t) = \hat{u}_{h=20}(t) - u_{h=0}(t)$ between the solutions computed with the biased and the exact models. The mean value of this bias $b_u(t)$ is evident at the end of the time interval.

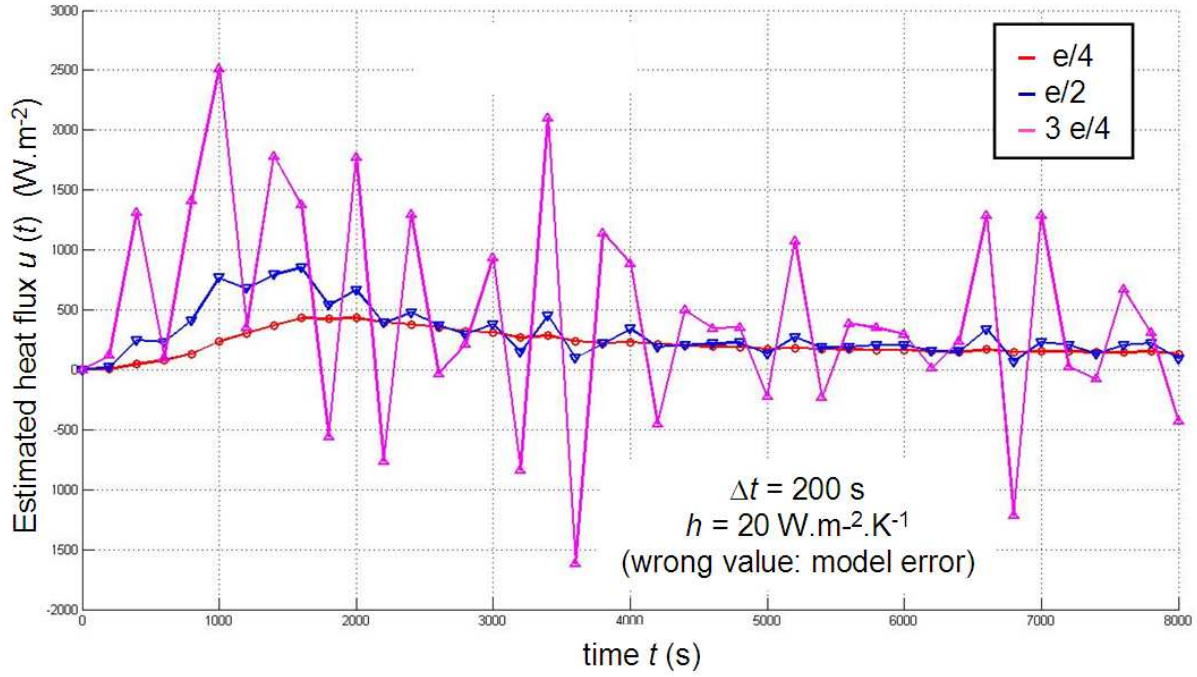

Figure 9e –Estimated heat flux $\hat{u}_{h=20}(t)$ with a biased model **(***h* = 20 W m^{-2} K^{-1} , instead of *h* = 0);
$\Delta t = 200$ s ; $\sigma = 0{,}02\ K$

3.4- The IHCP in a plane wall – Effect of a multi sensor output

Some improvements are obtained by considering simultaneously the output signals of several sensors.

- With only one sensor, the matrix S in the observation equation $\mathbf{y}_{mo} = \mathbf{S}\,\mathbf{u}$, is squared.
- With two sensors, the size of the matrix ***C***, equation xxx, becomes size(***C***)= (*2 x n)* and the size of the output signal vector is size(*y) = 2n*, then ***S*** is rectangular and size(***S***) = (2 *n x n*), so the inversion process has to be done in the least squared sense

$$(\mathbf{S}^T\mathbf{S})\,\mathbf{u} = \mathbf{S}^t\mathbf{y} \qquad \Rightarrow \qquad \hat{\mathbf{u}}_{OLS} = (\mathbf{S}^T\mathbf{S})^{-1}\,\mathbf{S}^T\mathbf{y} \tag{19}$$

Numerical results plotted on figure 9f, show the solutions obtained with two sensors located at *z* = *e*/4 *et z* = *e*/2 with noisy data ($\sigma = 0{,}02\ K$) and a time step $\Delta t = 200$ s, the plots compare the heat flux computed

- with the exact model (*h* = 0),
- and with the biased model (*h* = 20),

By eliminating the output signal close to the boundary *z* = *e*, the estimated input heat flux is less sensitive to the noise, but the systematic error on the estimated heat flux remains significant when the model is biased.

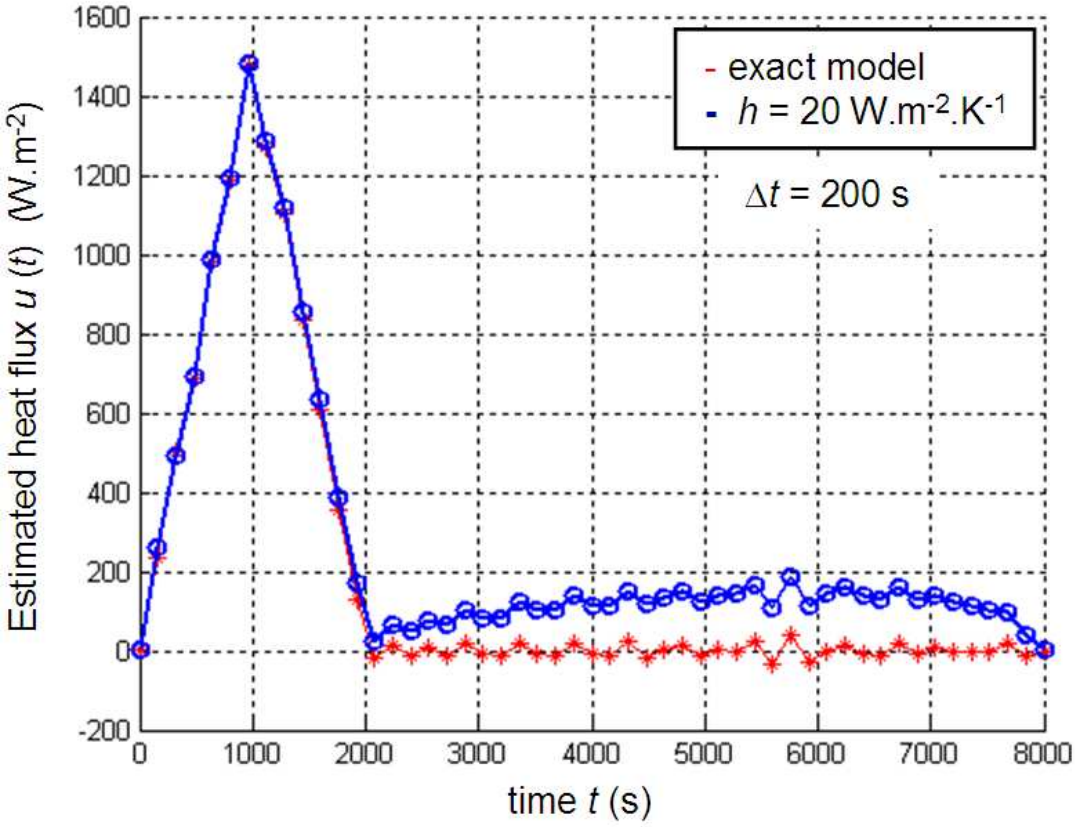

Figure 9f – Estimated input heat flux from combined output noisy data (σ= 0,02 K), given by two sensor located at z = e/4 et z = e/2 .

To avoid such situation, it is recommended to decouple the estimation problem of the boundary condition at $z = 0$ from that occurring at $z = L$. It means that several sensors have to be installed within the wall.

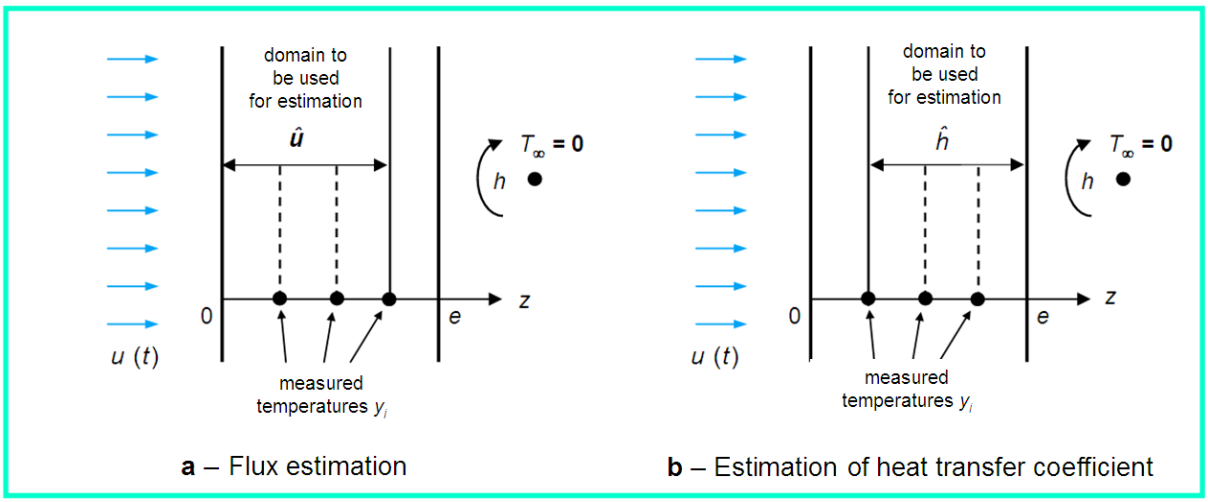

Figure 10 – Splitting the Inverse heat conduction problems for a plane wall case

For example, in the configuration including three sensors:

- To estimate $u(t)$ at $z = 0$, the model equation in the plane wall can be limited to the spatial domain $[z=0 , z=3e/4]$; the output signal at $z = 3e/4$ is then used to fix the boundary condition (Dirichlet condition); the inverse problem can be solved from the output data taken at $z=e/4$ and $z=e/2$, without knowing the heat transfer coefficient h,
- To estimate h at $z = L$, the model equation in the plane wall can be limited to the spatial domain $[z=e/4 , z=e]$; the output signal at $z = e/4$ is then used to fix the boundary condition (Dirichlet condition); the inverse problem can be solved from the output data taken at $z=e/2$ and $z=3e/4$, without knowing the heat flux $u(t)$ at $z = 0$.

More improvements could be done with a Bayesian approach [2]

4. Conclusion

In the analysis of heat conduction problem, the semi-infinite solid is a simple geometry that provides a useful idealization for many practical situations. A numerical solution of this inverse heat conduction problem has been easily investigated, thanks to the linearity of the model equation. The influence of variables like the noise level, the sensor locations, the time step on the instabilities of the non regularized solutions have been analyzed and illustrated. The SVD method is a powerful approach to control the regularized solutions.
For the linear heat conduction problem in a plane wall, a standard discretization of the spatial variable leads to a similar analysis of the instabilities of the numerical inverse problem solutions. Moreover the influence of a biased model, and the use of a multi-sensor output model have been illustrated.

References

[1] F P Incropera, D P DeWitt, *Fundamentals of Heat and Mass Transfer*, (IVth edition) John Wiley and Sons, New York, 1996
[2] D Maillet, Y Jarny and D Petit, *Problèmes inverses en diffusion thermique*, Techniques de l'Ingénieur", BE 8 266, Editions T.I., Paris, 2010
[3] Y Jarny and H Orlande, « *Adjoint Methods* », in "*Thermal Measurements in Heat Transfer*", CRC Press, 2011